Age-related Changes in the Hepatic Microcirculation in Mice

Yoshiya Ito[1], **Karen K. Sørensen**[2], **Nancy W. Bethea**[1], **Dmitri Svistounov**[2], **Margaret K. McCuskey**[1], **Bård H. Smedsrød**[2], and **Robert S. McCuskey**[1]

1 Department of Cell Biology and Anatomy, University of Arizona, Tucson, AZ 85724-5044

2 Department of Cell Biology and Histology, University of Tromsø, Tromsø, N-9037 Norway

Abstract

Aging of the liver is associated with impaired metabolism of drugs, adverse drug interactions, and susceptibility to toxins. Since reduced hepatic blood flow is suspected to contribute this impairment, we examined age-related alterations in hepatic microcirculation.. Livers of C57Bl/6 mice were examined at 0.8 (pre-pubertal), 3 (young adult), 14 (middle-aged) and 27 (senescent) months of age using *in vivo* and electron microscopic methods. The results demonstrated a 14% reduction in the numbers of perfused sinusoids between 0.8 and 27 month mice associated with 35% reduction in sinusoidal blood flow. This was accompanied by an inflammatory response evidenced by a 5-fold increase in leukocyte adhesion in 27 month mice, up-regulated expression of ICAM-1, and increases in intrahepatic macrophages. Sinusoidal diameter decreased 6-10%. Liver sinusoidal endothelial cell (LSEC) dysfunction was seen as early as 14 months when there was a 3-fold increase in the numbers of swollen LSEC. The endocytotic capacity of LSEC also was found to be reduced in older animals. The sinusoidal endothelium in 27 month old mice exhibited pseudocapillarization. In conclusion, the results suggest that leukocyte accumulation in the sinusoids and narrowing of sinusoidal lumens due to pseudocapillarization and dysfunction of LSEC reduce sinusoidal blood flow in aged livers.

1. Introduction

The liver plays a pivotal role in the metabolism of drugs and xenobiotics, the processing of physiological endogenous substances such as lipids, hormones, and different waste products, e.g., advanced glycation end products (AGEs), oxidatively modified low density lipoproteins (OxLDL), and material resulting from normal processes in connective tissue turnover, e.g., hyaluronan, chondroitin sulfate, and various collagen components (Smedsrod, 2004).

Aging of the liver is associated with reduction in its mass as well as a 30–40% reduction in blood flow (McLean and LeCouteur, 2004;Wynne et al., 1989). These changes are accompanied by impaired metabolism that have potential clinical implications including adverse drug reactions, susceptibility to toxins, and atherosclerosis due to spill-over of

Correspondence to: Robert S McCuskey, Ph. D, Department of Cell Biology and Anatomy, College of Medicine, PO BOX 245044, University of Arizona, 1501 N. Campbell Avenue, Tucson, AZ, 85724-5044, TEL: 520-626-6086, FAX: 520-626-2097, E-mail: mccuskey@email.arizona.edu

atherogenic molecules into the systemic circulation (LeCouteur et al., 2005;Schmucker, 2005). The reason(s) for this age related reduction in hepatic blood flow remains unknown and is puzzling since it has been concluded that there are few significant structural or biochemical changes in the aging liver (Jansen, 2002;Popper, 1986). More recently, however, Le Couteur et al (LeCouteur et al., 2001) have reported that in rats there are significant age associated reductions in the fenestration of liver sinusoidal endothelial cells (LSECs), increased expression of von Willebrand's factor, and increased deposition of extracellular matrix, basal lamina, and connective tissue elements in the Space of Disse leading to early capillarization or "pseudocapillarization" of the sinusoids in rats (LeCouteur et al., 2002). The same group has shown similar age-related alterations in LSEC in mice (Warren et al., 2005), baboons (Cogger et al., 2003) and humans (McLean et al., 2003). However, earlier studies failed to identify these changes (DeLeeuw et al., 1990;Schmucker, 1990). In addition, the one very limited study on the effects of aging on the liver microcirculation using *in vivo* microscopic methods (Vollmer et al., 2002), reported no significant changes in sinusoidal perfusion between young adult and old rats. Therefore, to date, there are few reports that confirm age-related changes in the hepatic microvasculature.

Advanced glycation end products (AGEs) are heterogeneous compounds resulting from non-enzymatic, irreversible glycation/glycoxydation of proteins and other biomolecules (Singh et al., 2001;Thornally, 1998). Such modifications lead to alterations in protein structure which in turn affect their physiological properties and make them resistant to lysosomal degradation. Accumulation of AGEs may have several pathological consequences such as: (a) quenching of NO with subsequent vasoconstriction and ischemia; (b) stimulation of cell signalling via RAGE resulting in the release of proinflammatory mediators, growth factors and adhesion molecules; stimulation of extracellular matrix synthesis and basal membrane thickening; and (c) free radical formation and increased oxidative stress (Basta et al., 1989;Bucaia et al., 1991;Fehrenbach et al., 2001;Simm et al., 2004).

Previously, we have reported that the liver is a principal site for removal of AGEs from the circulation, and that AGEs are exclusively eliminated by LSEC and Kupffer cells via scavenger receptors (Smedsrod et al., 1997). This clearance of AGEs and other modified macromolecules in the liver is important in preventing detrimental "spill-over" of these molecules into the systemic circulation. Such AGEs are known to be associated with diabetes mellitus, atherosclerosis, Alzheimer's disease and uremia. (Friedman, 1999;Hori et al., 1996;Kislinger et al., 1999;McCance et al., 1993;Schmidt et al., 1999;Sebkova et al., 1998). Normal aging is associated with an higher appearance of AGEs in various tissues and organs (Dunn et al., 1991;Hammes et al., 1999;Schleicher et al., 1997). The present study was conducted to identify age-related changes in the hepatic microvasculature and scavenger function using *in vivo* and electron microscopic methods.

2. Experimental procedures

2.1. Experimental animals

Male C57Bl6 mice were obtained from the National Institute of Aging (Bethesda, MD) and were specific pathogen free (SPF). The animals were placed in sterile, filter-topped cages containing sterile bedding, maintained in a 12 hr light/dark cycle, and allowed free access to sterilized NIH-31 mouse chow and water. The present study was performed in adherence to the National Institutes of Health guidelines for the use of experimental animals and followed the protocol approved by the Animal Care and Use Committee of the University of Arizona.

2.2. In vivo microscopy

Animals were anesthetized with urethane (2 mg/g b.w., subcutaneously). The hepatic microvascular responses were examined using established high resolution *in vivo* microscopic methods (McCuskey, 1986). Briefly, a compound binocular microscope (Leitz, Wetzlar, Germany) adapted for *in vivo* microscopy was equipped to provide either transillumination or epi-illumination as well as video microscopy using a charge-coupled device (CCD) camera (MTI, Michigan City, IN). With the water immersion objective (Leitz 80X/1.00, Wetzlar, Germany) employed for these studies, microvascular events were observed and recorded for at least 30s for subsequent off-line analysis using a Sony Betacam video tape recorder (Sony Medical Electronics, Park Ridge, NJ).

Kupffer cell function was assessed by measuring the phagocytosis of fluorescent 1.0-μm latex particles (Fluoresbrite-fluorescent monodispersed polystyrene microspheres; Polysciences, Warrington, PA) by individual cells. The latex was diluted 1:10 with sterile saline and injected in a 0.1 ml volume through a mesenteric vein using a 30 gauge lymphangiography needle (Becton Dickinson and Co., Franklin Lakes, NJ). The distribution and relative number of phagocytic Kupffer cells was measured by counting the number of cells that phagocytosed latex particles in a standardized microscopic field (4,125 μm^2) 15 min after each mice had received the injection of latex. To assess regional distribution, the number of phagocytic Kupffer cells per microscopic field was counted in 10 periportal and 10 centrilobular regions in each animal. The relative adequacy of blood perfusion through the sinusoids was evaluated by counting the number of perfused sinusoids in the same 10 microscopic fields in which the numbers of phagocytic Kupffer cells were determined. Because reduced perfusion of individual sinusoids can limit the delivery of the latex particles to Kupffer cells in these vessels, the ratio of Kupffer cells that phagocytosed latex particles to sinusoids containing flow was used as an overall index of Kupffer cell phagocytic activity.

To examine the interaction of leukocytes with the sinusoidal wall, quantification of leukocytes adhering to the endothelial lining of sinusoids was calculated by counting the number of leukocytes per unit length of sinusoid (adherent leukocytes/100 μm) in the same microscopic fields. A leukocyte was defined as adhering to the sinusoidal wall if it remained stationary for at least 30 secs. Endothelial swelling, which is thought to be an indicator of activation and/or injury, was assessed by counting the numbers of endothelial cells whose nuclear regions protrude across one third or more of the lumen in the same microscopic field. The results were averaged, and the data were represented as the average number in each animal.

Another set of experimental animals was used to assess the functional integrity of LSEC. Formaldehyde-treated serum albumin (FSA) labeled with tri-rhodamine isothiocyanate (TRITC) (6 mg/ml, 0.1 ml) or TRITC-AGE (8.6 mg/ml, 0.1 ml) was injected through a mesenteric vein as previously reported (Ito et al., 2003). FSA was prepared as described by (Mego et al., 1967). AGE-bovine serum albumin (AGE-BSA) was prepared as follows. BSA (50 mg/ml, Sigma, 99% purity, essentially fatty acid and globulin free) was incubated with 75 mM glucose in 0,33M disodium hydrogen phosphate/NaOH buffer (pH 11) for 2 wk at 50°C. Non-incorporated glucose was removed by dialysis against PBS under sterile conditions using regenerated cellulose dialysis membrane with MWCO 25,000 Da. TRITC-AGE and –FSA were prepared by incubating tri-rhodamine B isothiocyanate and AGE-BSA or FSA in sodium carbonate buffer (0.5 mol/l, pH 9.5) in a protein:dye ratio of 4:1 at 4°C overnight. Unreacted dye was removed by filtration through a PD-10 column (Sephadex G-25, Amersham Pharmacia Biotech, Uppsala, Sweden) equilibrated and eluted with PBS.

To test the effect of AGE on subsequent endocytosis of another scavenger receptor ligand, a saturation dose of AGE-BSA (8.6 mg/ml, 0.1 ml) was injected through a mesenteric vein followed 10 min later by injection of TRITC-FSA (6 mg/ml, 0.1 ml) and the uptake of the latter

monitored by *in vivo* microscopy. The saturation dose was determined by injecting 10, 100, and 500 μgm ^{125}I –labeled AGE-BSA intravenously into the tail vein of other C57Bl6 mice, and measuring rate of blood clearance during a one hour period as well as the radioactive uptake in organs and carcass after 1 hr. Saturation was obtained with the 500 μgm dose.

2.3. Laser Doppler flowmeter

Sinusoidal blood flow (erythrocyte flux) was measured by laser Doppler flowmetry (LDF) using a laser Doppler flowmeter (Moor Instruments, Wilmington, DE). A microprobe (P5a/P5b) was placed on the surface of the left lobe of the livers. The LDF signal is digitized with Moor Lab software (Moor Instruments) and sinusoidal blood flow was expressed in arbitrary units (Wheatley et al., 1993).

2.4. Electron microscopy

In a separate set of experimental animals (3 mice/group), routine methods were used to prepare liver specimens for transmission (TEM) and scanning (SEM) electron microscopy (McCuskey, 1986;McCuskey and McCuskey, 1990). Briefly, the livers are perfused through the portal vein with 0.1 M Na-cacodylate buffer to aid in washing out blood. This is immediately followed with a fixative containing 1.5% glutaraldehyde in 0.1 M cacodylate buffer, pH 7.4. For TEM, minced pieces of liver are further fixed for 2 hrs, then washed in buffer, postfixed with 1% osmium tetroxide in 0.1 M cacodylate buffer at 4°C, dehydrated through graded alcohols, briefly rinsed in propylene oxide and embedded in Epon. Thin sections are cut on a Reichert Ultracut microtome, examined using a Philips CM-12S electron microscope and recorded using an AMT-XR40, 2K × 2K CCD camera and AMT software. The same software was used to measure the thickness of 10 midlobular sinusoidal endothelium at 10 points in each liver at a magnification of 7100X.

For SEM, pieces of perfused-fixed livers are dehydrated in a graded ethanol series, critical point-dried, fractured, sputter-coated with 10 nm gold and examined using a Philips XL35 scanning electron microscope. Images of 5 periportal and 5 centrilobular sinusoids are recorded digitally at 8000X and the numbers of fenestrae/100 μm counted.

2.5. Histology

Formalin-fixed tissue samples (3 mice/group) were embedded in paraffin and sectioned at 5-μm. Liver sections were stained with the naphthol AS-D chloroacetate esterase technique for evaluation of neutrophil infiltration in mouse livers. Sirius Red was used to stain for collagen.

Immunohistochemistry was performed using antibodies for F4/80 (Serotec, Raleigh, NC), and intercellular adhesion molecule (ICAM)-1 (BD Sciences Pharmingen, Palo Alto, CA) to identify respectively Kupffer cells plus other intrahepatic macrophages and the expression of ICAM-1. After deparaffinization and rehydration, the endogenous peroxidase was quenched with .3% H_2O_2. This was followed by incubation with a protein block (DAKO Corporation, Carpinteria, CA). The sections were then incubated with the primary antibody, anti-F4/80 (1:50) or anti-ICAM-1 (1:300) overnight. The specificity of the reaction was verified using isotype-matched immunoglobulin antibody, rat IgG or hamster IgG in the same manner. Reaction products were visualized using streptavidin-biotin peroxidase kit (DAKO).

2.6 Statistical analysis

All data are expressed as means ± SEM. Multiple comparisons were preformed using Kruskel-Wallis one-way ANOVA on ranks with a Holm-Sidak Test. Differences were considered significant for p values less than 0.05.

3. Results

3.1. Effect of aging on hepatic microcirculation and sinusoidal endothelial cell function

Table 1 summarizes age-related changes in hepatic microcirculation. Sinusoidal blood flow in 27 month old mice was significantly decreased by 35% when compared with 0.8 month old mice. This was accompanied by decreased numbers of perfused sinusoids (15%) as well as diameters of the sinusoids (10%), and by increased adherence of leukocytes (5-fold). The numbers of swollen endothelial cells was increased (3-fold) as early as 14 months. These microvascular events were associated with hepatic recruitment of neutrophils and macrophages (Fig. 1). Accumulation of inflammatory cells into the aged livers was associated with increased expression of ICAM-1 in the walls of the sinusoids (Fig. 1). Kupffer cell phagocytic activity in centrilobular regions was reduced after puberty (50–60% reduction compared to 0.8 month old mice), but then remained almost unchanged up to old age. In contrast, periportal activity was slightly reduced at 3.3 and 14 months, but returned toward 0.8 month levels in the oldest animals.

The endocytosis of saturation doses of TRITC-FSA, a ligand for the scavenger receptors on LSEC was decreased at 14 months and was further reduced at 27 months, particularly in the centrilobular regions, when compared with 0.8 month old mice (Fig. 2). The endocytosis of saturation doses of TRITC-AGE, another ligand for these receptors, similarly was reduced at 27 months (Fig. 3). Pretreatment with a saturation dose of AGE also suppressed the endocytosis of TRITC-FSA by SECs (Fig. 4) indicating competition for uptake by the same receptors.

Stellate cells at 27 months contained numerous lipid droplets.

3.2 EM studies

TEM studies showed minimal changes in the sinusoids in mice at 0.8, 3.3 and 14 months old (Figs 5A, B, C). In contrast, the presence of basal laminae and collagen deposition was clearly evident in the Space of Disse in the livers from 27 month old mice (Figs 5D, E) and confirmed the light microscopic demonstration of scattered perisinusoidal collagen deposition in sections stained with Sirius Red (Fig. 6). The sinusoidal endothelium also was thickened in the 27 month old mice (Table 2). Hepatic stellate cells contained abundant lipid droplets (Fig. 5F).

SEM studies demonstrated fenestration organized in sieve plates in 0.8, 3.3 and 14 month old mice (Fig. 7A and B); there was less fenestration in the endothelium of the sinusoids in 27 month old mice (Fig. 7C, Table 2). There were no statistically significant differences in this loss of fenestration between periportal and centrilobular sinusoids (data not shown). As a result, the data from both sites were combined (Table 2).

4. Discussion

4.1. Age-related changes in liver microcirculation in mice

Reduced hepatic blood flow in the elderly has been suggested to be the major effect of aging on the liver circulation (McLean and LeCouteur, 2004;Wynne et al., 1989). Only a few studies have reported age-related structural and functional changes in the hepatic microvasculature. Recently, LeCouteur and co-workers have revealed the age-related changes in LSECs (Cogger et al., 2003;Hilmer et al., 2005;LeCouteur et al., 2001;McLean et al., 2003;Warren et al., 2005).

The present study demonstrated that hepatic microcirculatory dysfunction occurs in the aged mouse liver. Age-related changes in the hepatic microcirculation include impairment of sinusoidal blood flow associated with leukocyte-endothelial interactions and accumulation of

macrophages suggestive of an hepatic microvascular inflammatory response (McCuskey, 1993). Leukocyte accumulation into the liver of aged mice resulted, at least in part, from increased expression of ICAM-1 in the sinusoid lining further suggesting an age-related inflammatory response. This is consistent with reports of an age-related up-regulation of the inflammatory response (Licastro et al., 2005). Reduced width of the hepatic sinusoids and swollen LSEC in old mice also contributed to trapping leukocytes and sinusoidal obstruction resulting in impaired sinusoidal perfusion.

The phagocytic function of centrilobular Kupffer cells decreased after puberty and then was rather stable up to old age. In the periportal regions, Kupffer cell phagocytic activity also decreased after puberty, but increased to pre-pubertal levels in the oldest mice which may be related to the increased numbers of macrophages in the liver. Some of these results are in contrast to the single report in the literature on the hepatic microcirculation during aging in rats (Vollmer et al., 2002) which reported no change in leukocyte adhesion to the sinusoids, the diameters of the sinusoids, and Kupffer cell phagocytic function. However, the numbers of perfused sinusoids was decreased in old rats, which is consistent with our results. The different results may be due to the different methodologies, animal species, or different age groups.

Electron microscopic studies also demonstrated an age-related loss of fenestration in LSEC together with thickening of the endothelium, formation of basal lamina, and collagen deposition in the Space of Disse, These findings are in agreement with those recently reported in aged mice (Warren et al., 2005) as well as in rats (Hilmer et al., 2005;LeCouteur et al., 2001), baboons (Cogger et al., 2003), and humans (McLean et al., 2003). These age-related structural changes in LSEC and in the Space of Disse have been termed "pseudocapillarization" by LeCouteur (LeCouteur et al., 2002) and may reflect early capillarization stimulated by age-related low grade inflammation (Licastro et al., 2005). The formation of basal lamina and collagen deposition in the Space of Disse appear to contribute to the narrowing the lumen of the sinusoids and to impaired sinusoidal perfusion. Functionally, this pseudocapillarization in the liver also is thought to restrict blood-parenchymal exchange. Hilmer et al (Hilmer et al., 2005) have shown reduced diffusion of small lipoproteins in aged rat livers.

4.2. Effect of aging on the scavenger function of sinusoidal endothelial cells

The early capillarization depresses not only sieving function of LSEC but also may affect endocytotic activity. LSECs play a critical role in the endocytotic removal of blood borne soluble macromolecular waste products (Seternes et al., 2002), like AGEs and other modified proteins and lipoproteins and different products from extracellular matrix turnover. Indeed, the present study showed suppressed endocytotic capacity in the old mice, especially in the centrilobular region, suggesting compromised scavenger function in aging SEC and an age-related reduction in this important clearance function. This may increase the risk of extrahepatic deposition and deleterious effects of circulating waste macromolecules. Such circulating AGEs are known to be associated with diabetes mellitus, atherosclerosis, Alzheimer's disease and uremia. (Friedman, 1999;Hori et al., 1996;Kislinger et al., 1999;McCance et al., 1993;Schmidt et al., 1999;Sebkova et al., 1998). Pretreatment of young adult mice with AGE-BSA suppressed the subsequent endocytosis of TRITC-FSA in LSEC, indicating uptake by the same receptors, as has been reported earlier in vitro (Smedsrod et al., 1997). Uptake of AGEs in SEC also may lead to a reduction in SEC endocytosis by other mechanisms. We have reported earlier that pre-incubation of isolated LSEC with AGEs, but not other ligands for the scavenger receptor such as FSA or hyaluronan, down-regulates scavenger receptor mediated endocytosis (Hansen et al., 2002) which led us to speculate that a continuous exposure of LSEC to circulating AGEs during a life-time leads to changes in the endocytotic capacity of the cells, resulting in spillover into the systemic circulation. However, given the 10 min period between administration of

AGE and the TRITC-FSA in the present study, we can not exclude the possibility that the inhibition is due to a pure ligand-receptor competition.

In summary, we have demonstrated significant age-related changes in the hepatic microvasculature in mice, including the development of an hepatic microvascular inflammatory response and early capillarization in aged livers with reduced sinusoidal diameters resulting in a reduction in sinusoidal blood flow. We also found an age-related reduction in endocytotic capacity of the sinusoidal endothelium, especially in centrilobular regions. Whether the two are related currently is being investigated.

References

Basta M, Kirshbom P, Frank MM, Fries LF. Mechanism of therapeutic effect of high-dose intravenous immunoglobulin. Attenuation of acute, complement- dependent immune damage in a guinea pig model. J Clin Invest 1989;84:1974–1981. [PubMed: 2687331]

Bucaia R, Tracey KJ, Cerami A. Advanced glycosylation products quench nitric oxide and mediate defective endothelium-dependent vasodilatation in experimental diabetes. JClin Invest 1991;87:432–438. [PubMed: 1991829]

Cogger VC, Warren A, Fraser R, Ngu M, McLean AJ, LeCouteur DG. Hepatic sinusoidal pseudocapillarization with aging in the non-human primate. Exp Gerontol 2003;38:1101–1107. [PubMed: 14580863]

DeLeeuw MA, Brouwer A, Knook DL. Sinusoidal endothelial cells of the liver: Fine structure and function in relation to age. J Electron Microsc Tech 1990;14:218–236. [PubMed: 2187063]

Dunn JA, McCance DF, Thorpe SR, Lyons TJ, Baynes JW. Age- dependent accumulation of N epsilon-(carboxymethyl)lysine and N epsilon- (carboxymethyl)hydroxylysine in human skin collagen. Biochem 1991;30:1205–1210. [PubMed: 1899338]

Fehrenbach H, Weiskirchen R, Kasper M, Gressner AM. Up-regulated expression of the receptor for advanced glycation end products in cultured rat hepatic stellate cells during transdifferentiation to myofibroblasts. Hepatol 2001;34:943–952.

Friedman EA. Advanced glycosylated end products and hyperglycemia in the pathogenesis of diabetic complications. Diabetes Care 1999;22:B65–B71. [PubMed: 10097902]

Hammes HP, Hoerauf H, Alt A, Schleicher E, Clausen JT, Bretzel RG, Laqua H. N (epsilon) (carboxymethyl)lysin and the AGE receptor RAGE colocalize in age-related macular degeneration. Invest Ophthalmol Visual Sci 1999;40:1855–1859. [PubMed: 10393061]

Hansen B, Svistounov D, Olsen R, Nagai R, Horiuchi S, Smedsrod B. Advanced glycation end products impair the scavenger function of rat hepatic sinusoidal endothelial cells. Diabetologia 2002;45:1379–1388. [PubMed: 12378378]

Hilmer SN, Cogger VC, Fraser R, McLean AJ, Sullivan D, Couteur DGL. Age-related changes in the hepatic sinusoidal endothelium impede lipoprotein transfer in the rat. Hepatol 2005;42:1349–1354.

Hori O, Yan SD, Ogawa S, Kuwabara K, Matsumoto M, Stern D, Schmidt AM. The receptor for advanced glycation end-products has a central role in vascular disease in diabetes mellitus. Nephrol Dial Transplant 1996;11:13–16. [PubMed: 9044300]

Ito Y, Machen NW, Abril ER, McCuskey RS. Early hepatic microvascular injury in response to acetaminophen toxicity. Microcirc 2003;10:391–400.

Jansen PL. Liver disease in the elderly. Best Pract Res Clin Gastroenterol 2002;16:149–158. [PubMed: 11977934]

Kislinger T, Fu C, Huber B, Qu W, Taguchi A, Du YS, Hofmann M, Yan SF, Pischetsrieder M, Stern D, Schmidt AM. N(epsilon)-(carboxymethyl)lysine adducts of proteins are ligands for receptor for advanced glycation end products that activate cell signaling pathways and modulate gene expression. J Biol Chem 1999;274:31740–31749. [PubMed: 10531386]

LeCouteur DG, Cogger VC, Markus AMA, Harvey PJ, Yin ZL, Ansselin AD, McLean AJ. Pseudocapillarization and associated energy limitation in the aged rat liver. Hepatol 2001;33:537–543.

LeCouteur DG, Fraser R, Cogger VC, McLean AJ. Hepatic pseudocapillarisation and atherosclerosis in ageing. Lancet 2002;359:1612–1615. [PubMed: 12047987]

LeCouteur DG, Fraser R, Hilmer S, Rivory LP, McLean AJ. The hepatic sinusoid in aging and cirrhosis: effects on hepatic substrate disposition and drug clearance. Clin Pharmacokin 2005;44:187–200.

Licastro F, Candore G, Lio D, Porcellini E, Colonna-Romano G, Franceschi C, Caruso C. Innate immunity and inflammation in ageing: a key for understanding age-related diseases. Immunity and Ageing 2005;2:8. [PubMed: 15904534]

McCance DF, Dyer DG, Dunn JA, Bailie KE, Thorpe SR, Baynes JW, Lyons TJ. Maillard reaction products and their relation to complications in insulin- dependent diabetes mellitus. J Clin Invest 1993;91:2470–2478. [PubMed: 8514859]

McCuskey, RS. Microscopic methods for studying the microvasculature of internal organs. In: Baker, CH.; Nastuk, WF., editors. Physical Techniques in Biology and Medicine Microvascular Technology. Academic Press; New York: 1986. p. 247-264.

McCuskey RS, McCuskey PA. The fine structure and function of Kupffer cells. J Electron Microsc Tech 1990;14:237–246. [PubMed: 2338588]

McCuskey RS. Hepatic microvascular responses to endotoxemia and sepsis. Prog Appl Microcirc 1993;19:76–84.

McLean AJ, LeCouteur DG. Aging biology and geriatric clinical pharmacology. Pharmacol Rev 2004;56:163–184. [PubMed: 15169926]

McLean AJ, Cogger VC, Chong GC, Warren A, Markus AMA, Dahlstrom JE, LeCouteur DG. Age-related pseudocapillarization of the human liver. J Path 2003;200:112–117. [PubMed: 12692849]

Mego JL, Bertini F, McQueen JD. The use of formaldehyde-treated [131]I- albumin in the study of digestive vacuoles and some properties of these particles from mouse liver. J Cell Biol 1967;32:699–707. [PubMed: 6034485]

Popper H. Aging and the liver. Prog Liver Dis 1986;8:659–683. [PubMed: 3520674]

Schleicher ED, Wagner E, Nerlich AG. Increased accumulation of the glycoxidation product N(epsilon)-(carboxymethyl)lysine in human tissues in diabetes and aging. J Clin Invest 1997;99:457–468. [PubMed: 9022079]

Schmidt AM, Yan SD, Wautier JL, Stern D. Activation of receptor for advanced glycation end products: a mechanism for chronic vascular dysfunction in diabetic vasculopathy and atherosclerosis. Circ Res 1999;84:489–497. [PubMed: 10082470]

Schmucker DL. Hepatocyte fine structure during maturation and senescence. J Electron Microsc Tech 1990;14:106–125. [PubMed: 2406386]

Schmucker DL. Age-related changes in liver structure and function: Implications for disease ? Exp Gerontol 2005;40:650–659. [PubMed: 16102930]

Sebkova K, Schinzel R, Ling H, Simm A, Xiang G, Gekle M, Munch G, Vamvakas S, Heidland A. Advanced glycated albumin impairs protein degradation in the kidney proximal tubules cell line LLC-PK1. Cell Mol Biol 1998;44:1051–1060. [PubMed: 9846887]

Seternes T, Sorensen K, Smedsrod B. Scavenger endothelial cells of vertebrates: A nonperipheral leukocyte system for high-capacity elimination of waste macromolecules. PNAS 2002;99:7594–7597. [PubMed: 12032328]

Simm A, Bartling B, Silber RE. RAGE: A new pleiotropic antagonistic gene? Ann NY Acad Sci 2004;1019:228–231. [PubMed: 15247020]

Singh R, Barden A, Mori T, Beilin L. Advanced glycation end-products: a review. Diabetologia 2001;44:129–146. [PubMed: 11270668]

Smedsrod B. Clearance function of scavenger endothelial cells. Comparative Hepatol 2004;(3 Suppl 1): 22.

Smedsrod B, Melkko J, Araki N, Sano H, Horiuchi S. Advanced glycation end products are eliminated by scavenger-receptor-mediated endocytosis in hepatic sinusoidal Kupffer and endothelial cells. Biochem J 1997;322:567–573. [PubMed: 9065778]

Thornally PJ. Cell activation by glycated proteins. AGE receptors, receptor recognition factors and functional classification of AGEs. Cell Mol Biol 1998;44:1013–1023. [PubMed: 9846883]

Vollmer B, Pradarutti S, Richter S, Menger M. In vivo quantification of ageing changes in the rat from early juvenile to senescent life. Liver 2002;22:330–341. [PubMed: 12296967]

Warren A, Bertolino P, Cogger VC, A J, McLean Fraser R, LeCouteur DG. Hepatic sinusoidal pseudocapilliarization in aged mice. J Gerontol 2005;38:1101–1107.

Wheatley AM, Almond NE, Stuart ET, Zhao D. Interpretation of the laser doppler signal from the liver of the rat. Microvas Res 1993;45:290–301.

Wynne HA, Cope LH, Mutch E, Rawlins MD, Woodhouse KW, James OF. The effect of age upon liver volume and apparent liver blood flow in healthy man. Hepatol 1989;9:297–301.
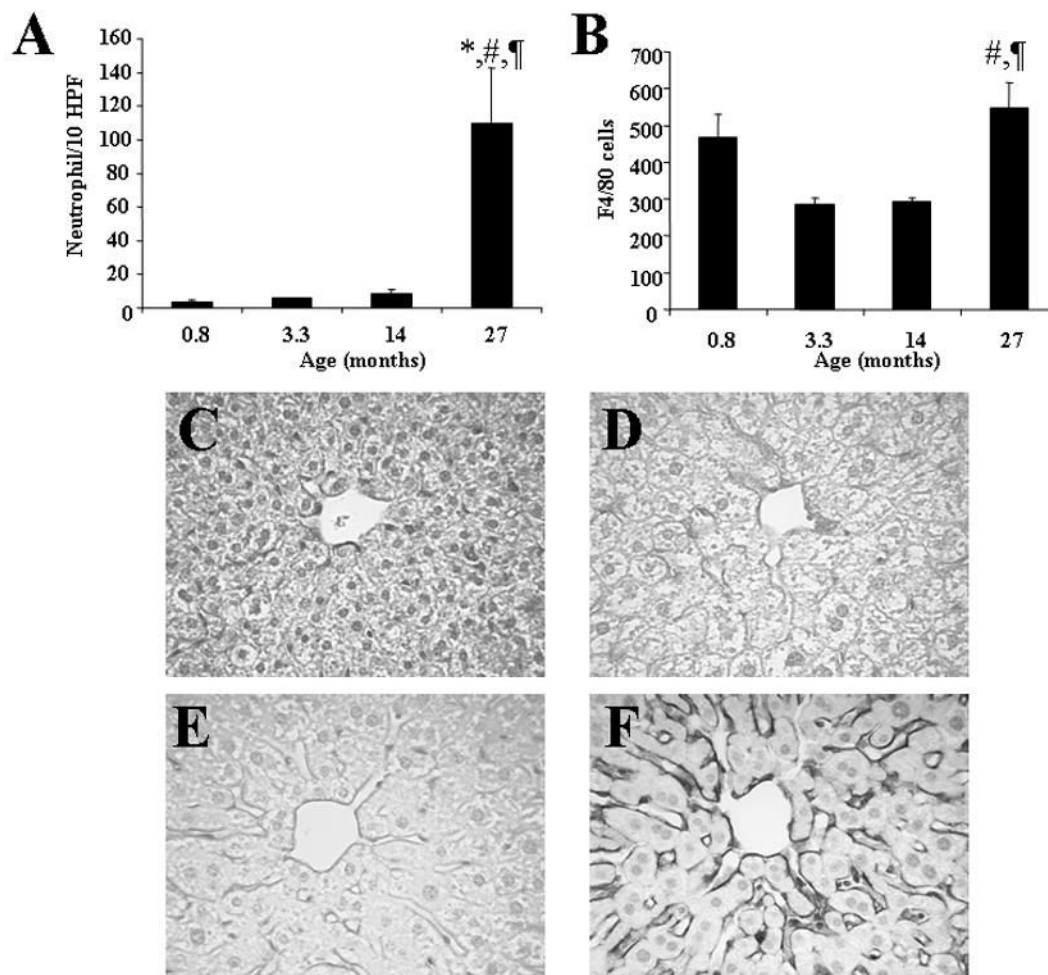
Figure 1.
The numbers of inflammatory cells including neutrophils (A) and macrophages (B) and the immunoreactivity with ICAM-1 in the liver (C–F). The expression of ICAM-1 was significantly increased along the hepatic sinusoids in 27 month old mice (F) when compared with 0.8 (C), 3.3 (D), and 14 month old mice (E). Data are means ± SE from 6 animals per group. *: p<0.05 vs. 0.8 month old mice, #: p<0.05 vs. 3.3 month old mice, ¶: p<0.05 vs. 14 month old mice. Original magnification, X400.
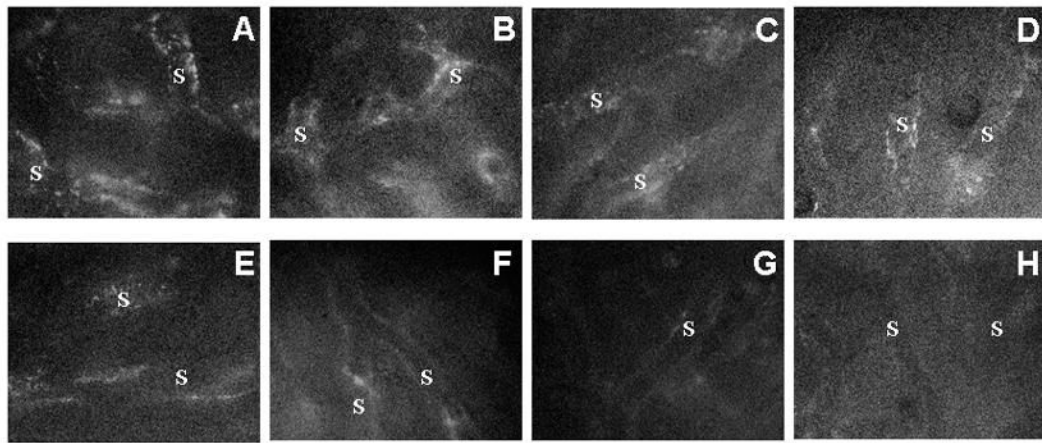
Figure 2.
Uptake of TRITC-FSA by the hepatic sinusoidal endothelium in 0.8 (A,E), 3.3 (B,F), 14 (C, G), and 27 (D, H) months old mice. The periportal sinusoids (A,B,C,D) and centrilobular sinusoids (E,F,G,H) were observed 30 min after the injection of TRITC-FSA. The uptake of TRITC-FSA was attenuated during aging. S: sinusoids. Original magnification, ×1,200.
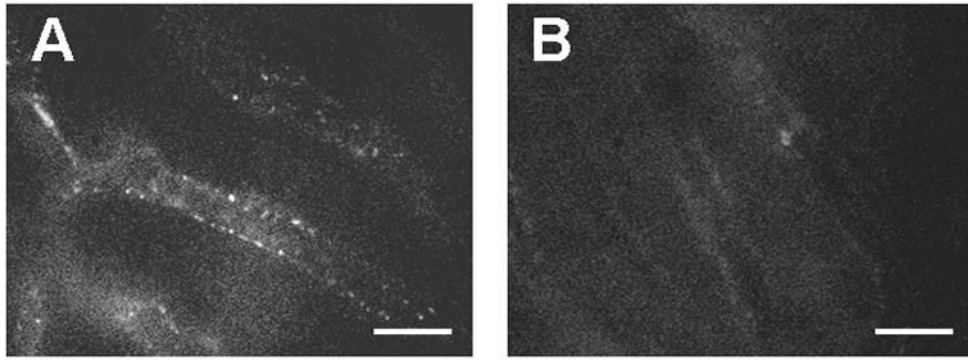
Figure 3.
Uptake of TRITC-AGE-BSA by the sinusoidal endothelium in the livers of 3.3 (A) and 27 (B) month old mice. TRITC-AGE-BSA was injected through a mesenteric vein 30 min before the observation of the liver microcirculation. The uptake of TRITC-AGE was suppressed in 27 month old mice when compared with 3.3 month old mice. Bars indicate 20 μm.
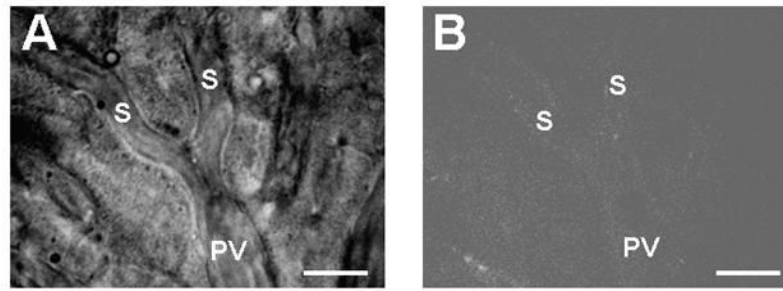
Figure 4.
Uptake of TRITC-FSA by the sinusoidal endothelium in livers from 3.3 month old mice pretreated with AGE-BSA. AGE-BSA was intraportally administered to mice 10 min before TRITC-FSA injection. Pretreatment with AGE-BSA suppressed subsequent FSA uptake by the sinusoidal endothelium. An epi-illumination image (right panel) is the same microcirculatory units obtained by transillumination (left panel). S, sinusoids; PV, portal venules. Bars indicate 20 μm.
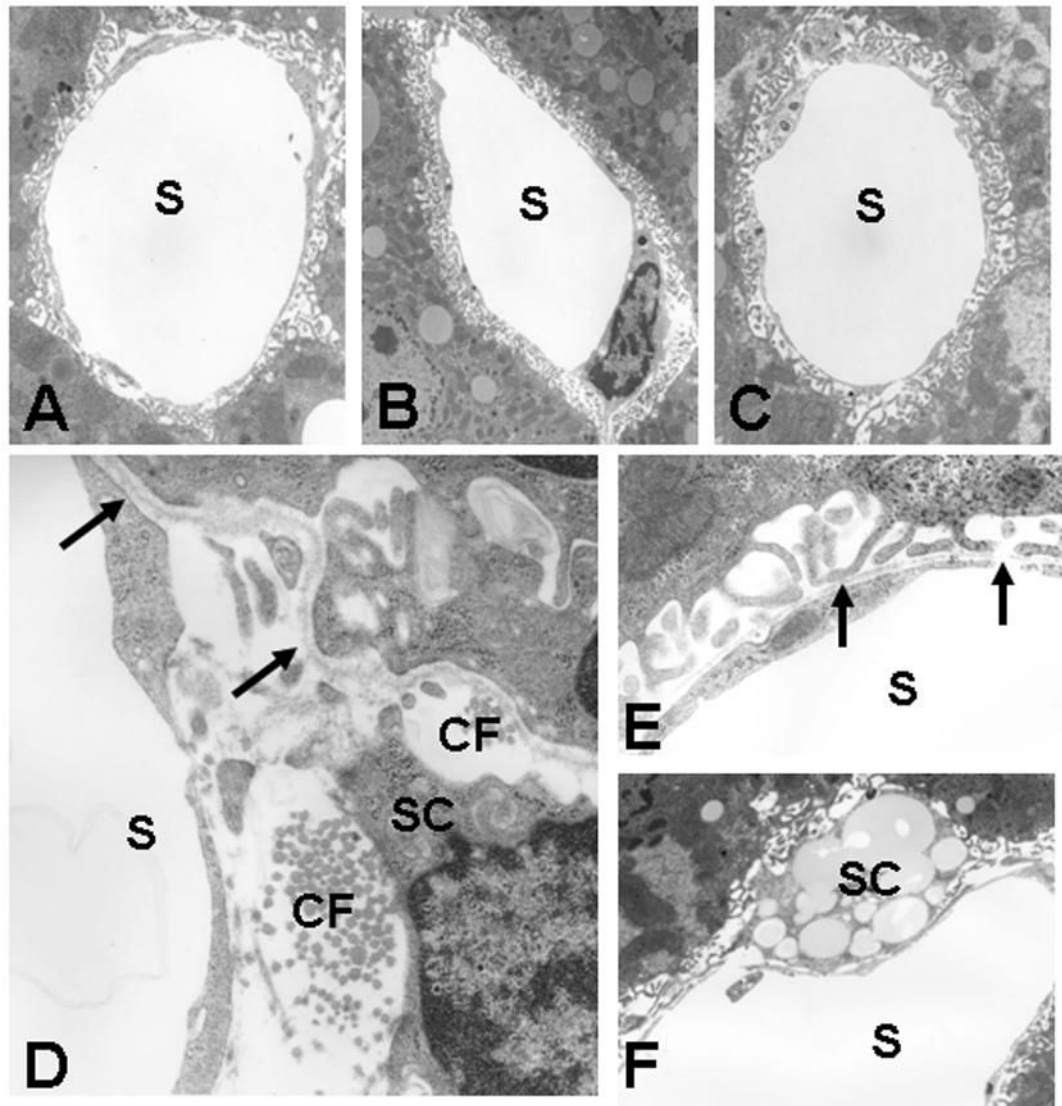
Figure 5.
Transmission electron micrographs of the sinusoids from the liver of 0.8 (A), 3.3 (B), 14 (C), and 27 (D,E,F) month old mice. In the liver from 0.8, 3.3, and 14 month old mice, the endothelium of the sinusoids was fenestrated and lacked a basal lamina (A,B,C). In contrast, in 27 month old mice, a subendothelial basal lamina (arrows) was formed and collagen fibrils (CF) were deposited in the space of Disse (D) (D, E). Hepatic stellate cells (SC) contained abundant lipid droplets (F). Original magnification, A, B, and C ×3,800; D and E, ×7,000; F, ×5,000.
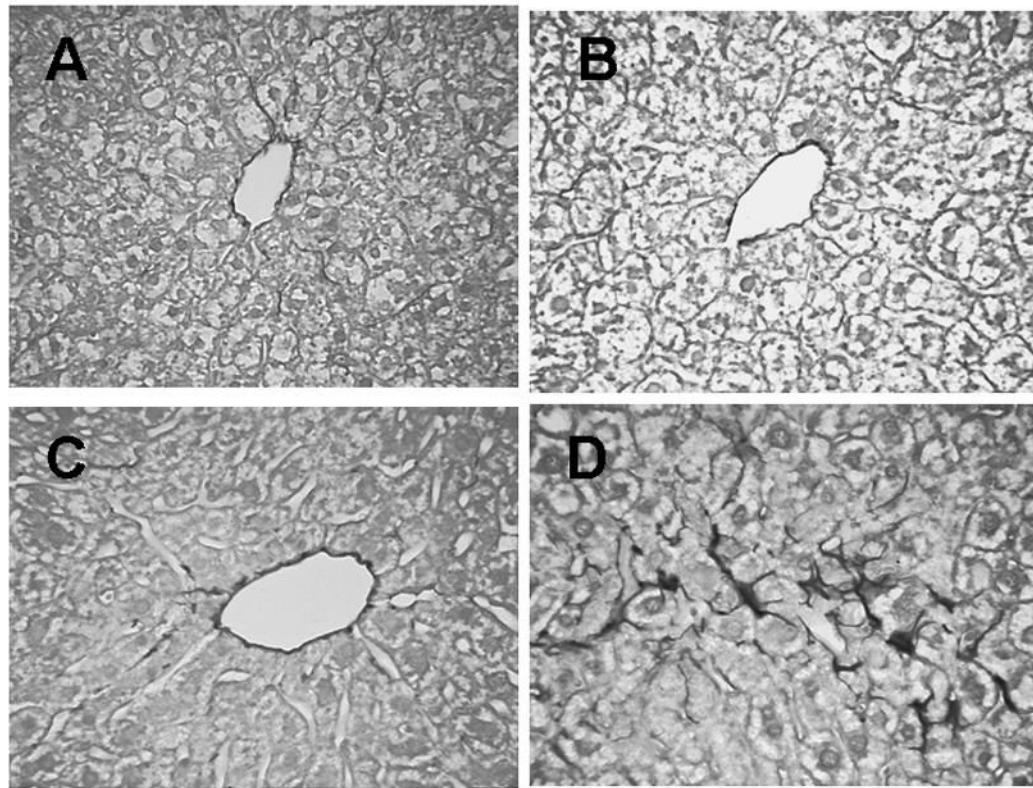
Figure 6.
Collagen staining with Sirius Red in 0.8 month (A), 3 month (B), 12 month (C), and 27 month (D) old mice. Arrows indicate darkly stained collagen principally around central venules in younger animals (A,B, C) with more in perisinusoidal locations in the 27 month old livers (D). ×400.
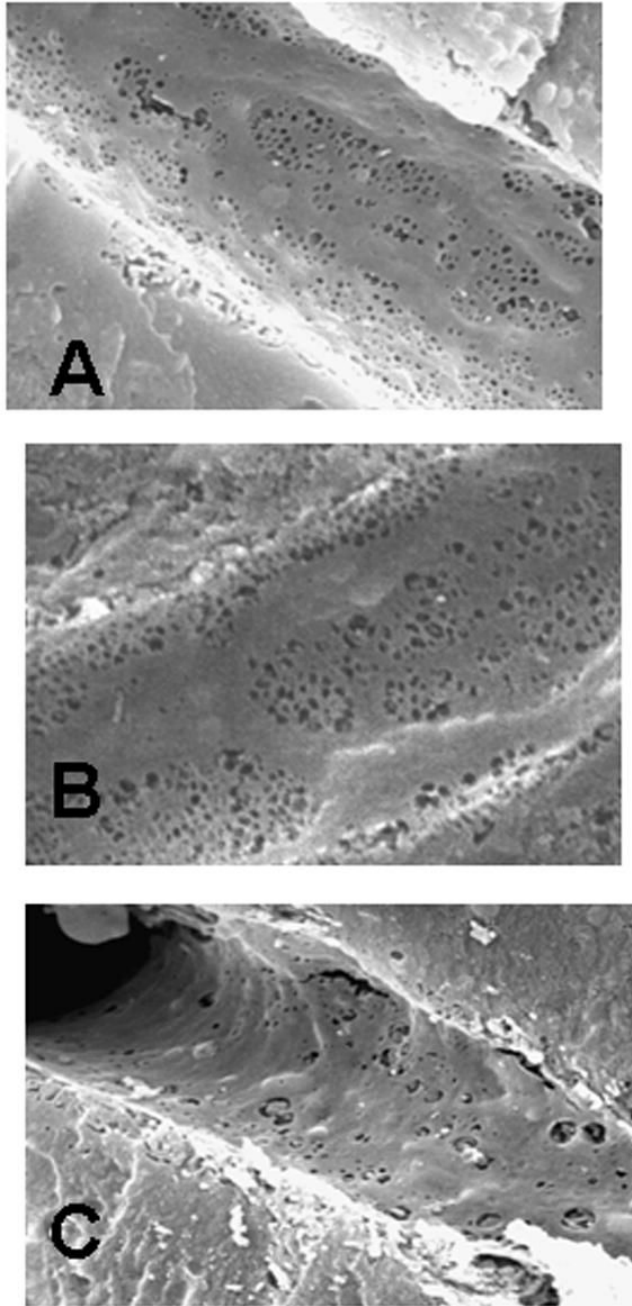
Figure 7.
Scanning electron micrographs of the sinusoids from the livers of 3.3 (A), 14 (B), and 27 (C) month old mice. The endothelium of the sinusoids from 3.3 and 14 month old livers (B, C) exhibited well developed fenestrated sieve plates. By 27 months there was a noticeable loss of fenestration (C). Original magnification, A and B, ×10,814; C, ×8,000.

Table 1

Effects of aging on liver microcirculation

	0.8 Mo	3.3 Mo	14 Mo	27 Mo
Laser Doppler flow (AU)	403.4±21.2	343.8±21.3	347.0±14.5	261.7±21.4,[ab]
Perfused sinusoids(/field)				
Periportal	4.8±0.1	4.9±0.1	4.6±0.1	4.1±0.1,[abc]
Centrilobular	4.4±0.1	4.5±0.1	4.3±0.1	4.0±0.1,[abc]
Swollen endothelial cells (/field)				
Periportal	0.3±0.1	0.2±0.0	0.3±0.1,[ab]	1.0±0.0,[ab]
Centrilobular	0.3±0.1	0.2±0.0	0.5±0.0,[ab]	0.6±0.1,[ab]
Adherent leukocytes (/100 μm)				
Periportal	0.06±0.01	0.03±0.01	0.04±0.01	0.29±0.01,[abc]
Centrilobular	0.09±0.02	0.05±0.01	0.04±0.01	0.21±0.01,[abc]
Kupffer cell phagocytic activity				
Periportal	0.99±0.06	0.69±0.05	0.66±0.04[a]	0.87±0.05,[bc]
Centrilobular	0.52±0.01	0.29±0.06[a]	0.21±0.06[a]	0.21±0.03[a]
Diameter of the sinusoids (μm)				
Periportal	5.9±0.1	5.6±0.1	5.7±0.1	5.4±0.0[a]
Centrilobular	7.2±0.1	6.8±0.1[a]	6.6±0.1[a]	6.5±0.2[a]

Data are the means ± SEM from 6–8 animals per group.

[a] $P < 0.05$ vs. 0.8 month old mice,

[b] $P < 0.05$ vs. 3.3 month old mice,

[c] P,0.05 vs. 14 month old mice.s

Table 2

Effects of aging on the sinusoidal endothelium

	0.8 Mo	3.3 Mo	14 Mo	27 Mo
Number of fenestrae (/50 μm2)	40.0 ± 2.69^{bcd}	130.94 ± 5.02^{bcd}	87.33 ± 3.51^{abd}	63.09 ± 3.96^{abc}
Thickness of the sinusoids (μm)	0.24 ± 0.01^{d}	0.23 ± 0.01^{d}	0.24 ± 0.01^{d}	0.38 ± 0.02^{abc}

Data are the means ± SEM from 3 animals per group.

[a] P<0.05 vs. 0.8 month old mice,

[b] P<0.05 vs. 3.3 month old mice,

[c] P<0.05 vs. 14 month old mice,

[d] P<0.05 vs. 27 month old mice.